Kinetic Studies on Reactions of Activated Triruthenium Carbonyl Clusters with Phosphorus Ligands†

Jian-Kun Shen and Fred Basolo*

Department of Chemistry, Northwestern University, Evanston, Illinois 60208-3113

Paul Nombel, Noël Lugan, and Guy Lavigne*

Laboratoire de Chimie de Coordination du CNRS, UPR 8241 liée par conventions à l'Université Paul Sabatier et à l'Institut National Polytechnique de Toulouse, 205, route de Narbonne, 31 077 Toulouse Cedex, France

Received July 28, 1995⊗

Reactions of the cluster complexes [PPN][$Ru_3(\mu_3\text{-}\eta^2\text{-Xpy})(CO)_9$] (**1**−**3**) (Xpy = 2-substituted pyridyl group; **1**, X = PhN; **2**, X = MeN; **3**, X = S) with phosphines in THF solution are described. Complex **1**, containing the 2-anilinopyridyl group, reacts with P(*n*-Bu)$_3$ or PPh_3 at room temperature to yield the addition product [PPN]-[$Ru_3(\mu\text{-}\eta^2\text{-PhNpy})(CO)_9$L] (**4a,b**) (**a**, L = P(*n*-Bu)$_3$; **b**, L = PPh_3). This adduct slowly loses either the phosphine or a CO ligand to give a mixture of the starting antecedent species and its monosubstituted derivative. The corresponding intermediate adducts are not seen with 2-(methylamino)pyridyl and 2-thiopyridyl complexes **2** and **3** which react with P(*n*-Bu)$_3$ to yield respectively the monosubstituted complex [PPN][$Ru_3(\mu_3\text{-}\eta^2\text{-MeNpy})(CO)_8$P-(*n*-Bu)$_3$] (**5a**) and the disubstituted complex [PPN][$Ru_3(\mu_3\text{-}\eta^2\text{-Spy})(CO)_7(P(n\text{-Bu})_3)_2$] (**6a**). Kinetic results for these reactions are reported. The reactions are first-order in complex and first-order in ligand concentrations. It is proposed that the initial step for these reactions is an associative nucleophilic attack of phosphine ligands on the metal atom accompanied by opening of the μ-X bridge bond to form the adducts [PPN][$Ru_3(\mu\text{-}\eta^2\text{-Xpy})$-$(CO)_9$L]. The rates of reaction increase in the order 2-MeNpy < 2-Spy < 2-PhNpy. The reactivity order of these complexes toward nucleophiles is discussed in terms of electronic effects of their ancillary ligands.

Introduction

Kaesz[1a] was the first to report that incorporation of coordinating nucleophile anions into ruthenium carbonyl cluster complexes is an efficient means to activate them toward substitution reactions.[1] Many of the early studies dealt with the promoter effects of halides, alkoxides, pseudohalides,[2] and hydride ions.[3] Research in this area has been logically extended to the use of amido or thiolato groups as promoters.[4] The current research activities on these systems are mainly driven by their potential uses as homogeneous catalysts or catalyst precursors.[5] Kinetic studies[6,7] have been instructive for further understanding of the promoter effect of these anions on the metal carbonyl clusters and the mechanisms by which these activated clusters may assist substrate transformations.

For example, studies[6] on ligand substitution reactions of complexes [$Os_3X(CO)_{10}L]^-$ (X = halides, L = CO, PPh_3) suggest that bridge formation of the halide anion between two neighboring metal atoms in the reaction transition state is the origin of anionic activation of the metal clusters. The formation of a bridged μ-X anion coordinatively saturates the reaction transition state, thus providing a low enthalpy of activation ($\Delta H^{\ddagger}$ =15−18 kcal/mol) for ligand displacement. Recent kinetic investigations[7] on reactions of alkynes with the triruthenium carbonyl halide clusters [PPN][$Ru_3(Cl)(CO)_{11-n}$] (n = 0, 1) and [PPN][$Ru_3(\mu_3\text{-I})(CO)_9$] show that [PPN][$Ru_3(Cl)(CO)_{11}$] reacts by first losing one of its CO ligands to form a bridged halide intermediate, followed by its reaction with alkynes. The reactivities of alkynes follow the order $C_4H_9C{\equiv}CH \geq PhC{\equiv}CH \gg C_2H_5C{\equiv}CC_2H_5 \geq PhC{\equiv}CPh$, with μ_3-halide complexes being more reactive than μ_2-halide complexes.

The syntheses of anionic amido and thiolato triruthenium complexes of general formula [PPN][$Ru_3(\mu_3\text{-}\eta^2\text{-Xpy})(CO)_9$] (**1**−**3**) (Xpy = 2-substituted pyridyl groups; **1**, X = PhN; **2**, X = MeN; **3**, X = S) were reported.[4] A structure of type **I** was established for the anilinopyridyl derivative [PPN][$Ru_3(\mu_3\text{-}\eta^2$-PhNpy)$(CO)_9$] (**1a**). The trappable CO adduct of the latter compound, formulated as [PPN][$Ru_3(\mu\text{-}\eta^2\text{-PhNpy})(CO)_{10}$], was

† Dedicated to Professor Harry B. Gray on his 60th birthday.

⊗ Abstract published in *Advance ACS Abstracts,* January 1, 1996.

(1) (a) Szostak, R.; Strouse, C. E.; Kaesz, H. D. *J. Organomet. Chem.* **1980**, *191*, 243. (b) Ford, P. C.; Rokicki, A. *Adv. Organomet. Chem.* **1988**, *28*, 139. (c) Lavigne, G.; Kaesz, H. D. In *Metal clusters in Catalysis*; Gates, B., Guczi, L., Knozinger, H., Eds.; Elsevier: Amsterdam, 1986; Chapter 4. (d) Lavigne, G. In *The Chemistry of Metal Clusters*; Shriver, D., Adams, R. D., Kaesz, H. D. Eds.; Verlag Chemie: Weinheim, 1990; Chapter 5, p 201.

(2) (a) Lavigne, G.; Kaesz, H. D. *J. Am. Chem. Soc.* **1984**, *106*, 4647. (b) Han, S. H.; Geoffroy, G. L.; Dombek, B. D.; Rheingold, A. L. *Inorg. Chem.* **1988**, *27*, 4355. (c) Anstock, M.; Taube, D. J.; Gross, D. C.; Ford, P. C. *J. Am. Chem. Soc.* **1984**, *106*, 3696. (d) Rivomanana, S.; Lavigne, G.; Lugan, N.; Bonnet, J.-J.; Yanez, R.; Mathieu, R. *J. Am. Chem. Soc.* **1989**, *111*, 8959. (e) Lillis, L.; Rokicki, A.; Chin, T.; Ford, P. C. *Inorg. Chem.* **1993**, *32*, 5040.

(3) (a) Taube, D. J.; Ford, P. C. *Organometallics* **1986**, *5*, 99. (b) Lavigne, G.; Lugangn, N.; Bonnet, J.-J. *Inorg. Chem.* **1987**, *26*, 2345.

(4) (a) Lugan, N.; Laurent, F.; Lavigne, G.; Newcomb, T. P.; Liimatta, E. W.; Bonnet, J.-J. *J. Am. Chem. Soc.* **1990**, *112*, 8607. (b) Lugan, N.; Laurent, F.; Lavigne, G.; Newcomb, T. P.; Liimatta, E. W.; Bonnet, J.-J. *Orgnaometallics* **1992**, *11*, 1351.

(5) (a) Lavigne, G.; Lugan, N.; Kalck, P.; Soulié, J.-M.; Lerouge, O.; Saillard, J.-Y.; Halet, J.-F. *J. Am. Chem. Soc.* **1992**, *114*, 10669. (b) Han, S. H.; Geoffroy, G. L.; Rheingold, A. L. *Inorg. Chem.* **1987**, *26*, 3428. (c) Dombek, B. D. *J. Am. Chem. Soc.* **1981**, *103*, 6508. (d) Dombek, B. D. *Organometallics* **1985**, *4*, 1707. (e) Zuffa, J. L.; Blohm, M. L.; Gladfelter, W. L. *J. Am. Chem. Soc.* **1986**, *108*, 552. (f) Lugan, N.; Lavigne, G.; Soulié, J.-M.; Fabre, S.; Kalck, P.; Saillard, J.-Y.; Halet, J.-F. *Organometallics* **1995**, *14*, 1713.

(6) Shen, J. K.; Basolo, F. *Organometallics* **1993**, *12*, 2942.

(7) Shen, J. K.; Basolo, F. *Gazz. Chim. Ital.* **1994**, *124*, 439.

0020-1669/96/1335-0755$12.00/0

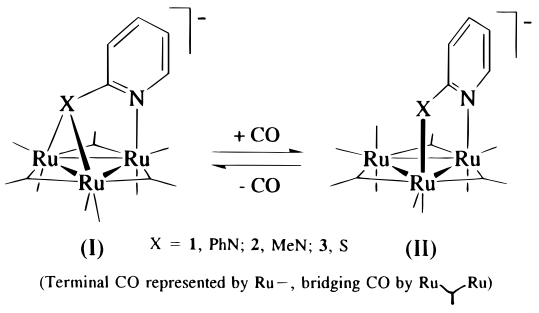

(I) X = **1**, PhN; **2**, MeN; **3**, S **(II)**

(Terminal CO represented by Ru−, bridging CO by Ru⟨Ru)

found to exhibit a structure of type **II**, analogous to the one established by X-ray diffraction for the closely related alkoxopyridyl derivative [PPN][$Ru_3(\mu\text{-}\eta^2\text{-Opy})(CO)_{10}$].[4]

The neutral hydrido complexes obtained by protonation of type I anionic derivatives are so reactive toward phosphines that intermediate adducts are not intercepted (PPh_2−H substitution is complete within 2 min at −40 °C).[4a] These complexes have also shown interesting catalytic properties for the hydrogenation of alkynes,[4a,8] and for various alkyne-based reactions including the codimerization of diphenylacetylene and ethylene,[4a] the polymerization of phenylacetylene, the synthesis of 1,4-bis(triphenylsilyl)but-1-en-3-yne, and the synthesis of α-phenylcinnamaldehyde *via* hydroformylation of diphenylacetylene.[9]

A kinetic study of reactions of type **I** species with phosphorus ligands was undertaken with the aim to evaluate the influence of the nature of the ancillary ligand on the reactivity of the cluster.

Experimental Section

Reagents. THF was distilled under N_2 from sodium benzophenone ketyl. The complexes [PPN][$Ru_3(\mu_3\text{-}\eta^2\text{-Xpy})(CO)_9$] (**1**−**3**) (**1**, X = PhN; **2**, X = MeN; **3**, X = S) were synthesized according to published procedures.[4b] P(*n*-Bu)$_3$ was distilled under N_2 from sodium before use. PPh_3 was recrystallized from ethanol. The kinetic studies were made under pseudo-first-order conditions, with the concentration of entering nucleophile in 10-fold excess or more.

Reaction of [PPN][$Ru_3(\mu_3\text{-}\eta^2\text{-PhNpy})(CO)_9$] (1) with P(*n*-Bu)$_3$ and PPh_3. Both phosphines react with [PPN][$Ru_3(\mu_3\text{-}\eta^2\text{-PhNpy})(CO)_9$] (**1**) in THF at room temperature to yield the same addition product [PPN][$Ru_3(\mu\text{-}\eta^2\text{-PhNpy})(CO)_9$L] (**4a,b**) (**a**, L = P(*n*-Bu)$_3$; **b**, L = PPh_3). These complexes were obtained as orange oils. They were found to undergo subsequent intramolecular transformation *via* loss of a ligand. Indeed, when the PPh_3 adduct **4b** was dissolved in THF, it converted partially to its unsubstituted antecedent **1** *via* loss of the phosphine and partially to the monosubstituted product *via* CO loss at higher temperatures (40−60 °C) as indicated by IR monitoring. The P(*n*-Bu)$_3$ adduct **4a** was found to be more stable than the corresponding PPh_3 adduct **4b**, though its slow conversion into a mixture of the unsubstituted antecedent compound and the corresponding monosubstituted complex was also observed upon prolonged heating at 60 °C. Experimental details for the preparation of **4a** are given below.

Preparation of [PPN][$Ru_3(\mu_3\text{-}\eta^2\text{-PhNpy})(CO)_9$(P(*n*-Bu)$_3$)] (4a). Crystals of the complex [PPN][$Ru_3(\mu_3\text{-}\eta^2\text{-PhNpy})(CO)_9$] (**1**) (650 mg, 0.51 mmol) were dissolved in 40 mL of THF in a Schlenk tube. One equivalent of P(*n*-Bu)$_3$ (130 μL, 0.51 mmol) was added, and the mixture was stirred at 23 °C. A rapid color change from yellow to orange was observed, whereas IR monitoring indicated the quantitative formation of a compound subsequently formulated as [PPN][$Ru_3(\mu\text{-}\eta^2\text{-PhNpy})$-$(CO)_9$P(*n*-Bu)$_3$] (**4a**). After 30 min, the solvent was evaporated. The resulting orange oil was triturated with hexane and washed several times with the same solvent. It was finally dried under vacuum, weighed, and characterized (640 mg, 0.437 mmol, 85% yield). Anal. Calcd for $Ru_3C_{68}H_{66}N_{33}O_9$: C, 55.73; H, 4.51; N, 2.87. Found: C, 55.72; H, 4.88; N, 2.58. Spectroscopic data for **4a**: IR (ν(CO), THF) 2020 (m), 1980 (vs), 1958 (s), 1940 (ms), 1910 (m), 1898 (m), 1830 (vw), 1782 (ms, br), 1766 (ms, br) cm^{-1}; ^{31}P NMR (acetone-d_6) δ 26.42 (s, PPN^+), 27.84 (s, P(*n*-Bu)$_3$).

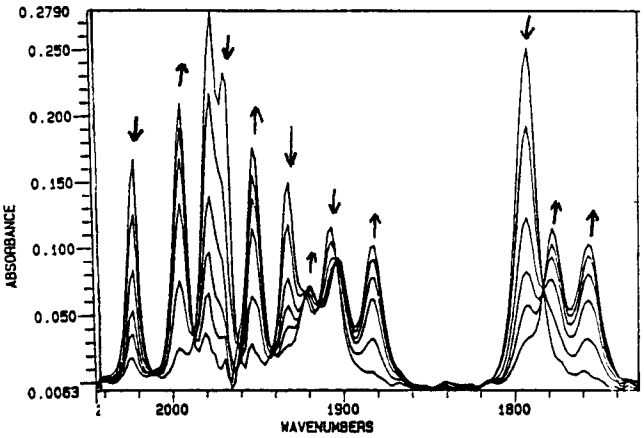

Figure 1. Infrared spectral changes with time (intervals of 4 min) for the reaction of [PPN][$Ru_3(\mu_3\text{-}\eta^2\text{-Spy})(CO)_9$] (**3**) with P(*n*-Bu)$_3$ (eq 3) at 12.4 °C in THF.

Reaction of [PPN][$Ru_3(\mu_3\text{-}\eta^2\text{-MeNpy})(CO)_9$] (2) with P(*n*-Bu)$_3$: Preparation of [PPN][$Ru_3(\mu_3\text{-}\eta^2\text{-MeNpy})(CO)_8$(P(*n*-Bu)$_3$)] (5a). Crystals of the complex [PPN][$Ru_3(\mu_3\text{-}\eta^2$-MeNpy)$(CO)_9$] (**2**) (200 mg, 0.166 mmol) were dissolved in 20 mL of THF in a Schlenk tube. One equivalent of P(*n*-Bu)$_3$ (45 μL, 0.166 mmol) was added, and the mixture was stirred at 23 °C. A progressive color change from yellow to red was observed, whereas IR monitoring indicated the spectroscopically quantitative formation of a new compound over a period of 2 h. After evaporation of the solvent, the resulting complex [PPN][$Ru_3(\mu_3\text{-}\eta^2$-MeNpy)$(CO)_8$P(*n*-Bu)$_3$] (**5a**) was isolated as a red oil (180 mg, 0.13 mmol, 79% yield). Spectroscopic data for **5a**: IR (ν(CO), THF) 1990 (vs), 1947 (s), 1915 (m), 1899 (ms), 1885 (ms), 1806 (vw), 1770 (ms), 1749 (ms) cm^{-1}; ^{31}P NMR (acetone-d_6) δ 25.73 (s, PPN^+), 27.03 (s, P(*n*-Bu)$_3$).

Preparation of [PPN][$Ru_3(\mu_3\text{-}\eta^2\text{-Spy})(CO)_8$(P(*n*-Bu)$_3$)] (5a$_1$). This monosubstituted derivative was prepared from [PPN][$Ru_3(\mu_3\text{-}\eta^2$-Spy)$(CO)_9$] (**3**) (250 mg) and 1 equiv of P(*n*-Bu)$_3$ under the same conditions as those described above for the isostructural MeNpy derivative **5a**. IR monitoring indicated the spectroscopically quantitative formation of a new compound over a period of 1 h. After evaporation of the solvent, the resulting complex [PPN][$Ru_3(\mu_3\text{-}\eta^2$-Spy)$(CO)_8$(P(*n*-Bu)$_3$)] (**5a$_1$**) was isolated as an orange oil (240 mg, 0.15 mmol, 70% yield). Spectroscopic data for **5a$_1$**: IR (ν(CO), THF) 1992 (vs), 1949 (s), 1918 (m), 1901 (ms), 1884 (ms), 1815 (vw), 1777 (ms), 1759 (ms) cm^{-1}; ^{31}P NMR (acetone-d_6) δ 25.72 (s, PPN^+), 29.02 (s, P(*n*-Bu)$_3$). ^{31}P NMR spectra revealed that the compound was contaminated by small amounts of the d-substituted derivative **6a**.

Preparation of [PPN][$Ru_3(\mu_3\text{-}\eta^2\text{-Spy})(CO)_7$(P(*n*-Bu)$_3$)$_2$] (6a). This disubstituted derivative was prepared from [PPN][$Ru_3(\mu_3\text{-}\eta^2$-Spy)$(CO)_9$] (**3**) (250 mg, 0.2 mmol) and 2 equiv of P(*n*-Bu)$_3$ (105 μL, 0.4 mmol). The solution was stirred for 90 min under slightly reduced pressure. The compound was isolated as a dark red oil (260 mg, 0.167 mmol, 80% yield). Anal. Calcd for $C_{72}H_{88}N_2O_7P_4Ru_3S_1$: C, 55.70; H, 5.71. Found: C, 56.06; H, 5.82. Spectroscopic data for **6a**: IR (ν(CO), THF) 1960 (vs), 1940 (sh), 1896 (ms), 1860 (m), 1746 (m) 1725 (s) cm^{-1}; ^{31}P NMR (acetone-d_6) δ 25.70 (s, PPN^+), 30.60 (s, 2 P(*n*-Bu)$_3$).

Kinetics. All kinetic experiments were run under pseudo-first-order conditions, with the concentration of the entering nucleophile in 10-fold excess or more. Kinetic data were obtained by following the disappearance of the ν(CO) bands of the reactant (Figure 1). The IR spectra were recorded on a Nicolet 5PC-FTIR spectrophotometer equipped with a P/N 20.5000 variable temperature IR cell with 0.6 mm spaced AgCl windows. Constant temperatures were obtained using a Neslab RTE-8 refrigeration circulating bath.

(8) (a) Cabeza, J. A.; Fernandez-Colinas, J. M.; Llamazares, A.; Riera, V. *Organometallics* **1993**, *12*, 4141. (b) Cabeza, J. A.; Fernandez-Colinas, J.; Llamazares, A.; Riera, V.; Garcia-Granda, S.; Van der Maelen, J. F. *Organometallics* **1994**, *13*, 4352. (c) Alvarez, S.; Briard, P.; Cabeza, J. A.; del Rio, I.; Fernandez-Colinas, J. M.; Mulla, F.; Ouahab, L.; Riera, V. *Organometallics* **1994**, *13*, 4360.

(9) Nombel, P.; Lugan, N.; Mulla, F.; Lavigne, G. *Organometallics* **1994**, *13*, 4673.

In a typical experiment, 0.5 mL of a 2×10^{-3} M THF solution of [PPN][$Ru_3(\mu_3\text{-}\eta^2\text{-Spy})(CO)_9$] (**3**) was mixed with 0.5 mL of a 0.5 M THF solution of P(*n*-Bu)$_3$ in a Schlenk tube which was kept at −78 °C. The mixed solution was then diluted with THF to 2 mL, and the solution was transferred with a syringe into an IR cell. After a few minutes for temperature equilibration, the IR spectral changes were recorded. Plots of 1n A_t (A_t is the absorbance of ν_{CO} of the reactant) vs time were linear over 2 half-lives ($r^2 > 0.995$) for all reactions. The slopes of these lines yield observed rate constants.

For the intramolecular ligand substitution of PPN[$Ru_3(\mu\text{-}\eta^2\text{-2-PhNpy})(CO)_9PPh_3$] (**4b**) (eqs 5 and 6), substitution of PPh_3 to form PPN[$Ru_3(\mu_3\text{-}\eta^2\text{-2-PhNpy})(CO)_9$] (**1**) is much faster than substitution of CO to form PPN[$Ru_3(\mu_3\text{-}\eta^2\text{-2-PhNpy})(CO)_8PPh_3$] (**5b**). The molar absorbance coefficient of **5b** was not obtained due to its low yield from the reaction. Thus, individual rate constants for the loss of PPh_3 (eq 5) and of CO (eq 6) were not obtained. The total rate constants ($k_5 + k_6$) were obtained by following the decrease of the CO-stretching band of the reactant, using $\ln(A_t - A_\infty) = k_{obsd}t + \text{constant}$, and are included in the supporting information, Table 2.

Results

Whereas reactions of [PPN][$Ru_3(\mu_3\text{-}\eta^2\text{-PhNpy})(CO)_9$] (**1**) with P(*n*-Bu)$_3$ or PPh_3 yield the addition product [PPN][$Ru_3(\mu\text{-}\eta^2\text{-PhNpy})(CO)_9L$] (**4a,b**) (**a**, L = P(*n*-Bu)$_3$; **b**, L = PPh_3) (eq 1), the complexes [PPN][$Ru_3(\mu_3\text{-}\eta^2\text{-MeNpy})(CO)_9$] (**2**) and [PPN][$Ru_3(\mu_3\text{-}\eta^2\text{-Spy})(CO)_9$] (**3**) react with P(*n*-Bu)$_3$ to yield directly the isostructural monosubstituted derivatives [PPN][$Ru_3(\mu_3\text{-}\eta^2\text{-MeNpy})(CO)_8(P(n\text{-Bu})_3)$] (**5a**) (eq 2) and [PPN][$Ru_3(\mu_3\text{-}\eta^2\text{-Spy})(CO)_8(P(n\text{-Bu})_3)$] (**5a$_1$**) (eq 3), respectively. The latter reacts with a second molecule of P(*n*-Bu)$_3$ to afford the disubstituted derivative [PPN][$Ru_3(\mu_3\text{-}\eta^2\text{-Spy})(CO)_7(P(n\text{-Bu})_3)_2$] (**6a**) (eq 4).

$$[Ru_3(\mu_3\text{-}\eta^2\text{-PhNpy})(CO)_9]^- + L \rightarrow \underset{\mathbf{1}}{} \underset{\mathbf{4a,b}\ (\mathbf{a} = L = P(n\text{-Bu})_3;\ \mathbf{b},\ L = PPh_3)}{[Ru_3(\mu\text{-}\eta^2\text{-PhNpy})(CO)_9L]^-} \quad (1)$$

$$[Ru_3(\mu_3\text{-}\eta^2\text{-MeNpy})(CO_9)]^- + P(n\text{-Bu})_3 \rightarrow \underset{\mathbf{2}}{} \underset{\mathbf{5a}}{[Ru_3(\mu_3\text{-}\eta^2\text{-MeNpy})(CO)_8(P(n\text{-Bu})_3)]^-} + CO \quad (2)$$

$$[Ru_3(\mu_3\text{-}\eta^2\text{-Spy})(CO)_9]^- + P(n\text{-Bu})_3 \rightarrow \underset{\mathbf{3}}{} \underset{\mathbf{5a_1}}{[Ru_3(\mu_3\text{-}\eta^2\text{-Spy})(CO)_8(P(n\text{-Bu})_3)]^-} + CO \quad (3)$$

$$[Ru_3(\mu_3\text{-}\eta^2\text{-Spy})(CO)_8(P(n\text{-Bu})_3)]^- + P(n\text{-Bu})_3 \rightarrow \underset{\mathbf{6a}}{[Ru_3(\mu_3\text{-}\eta^2\text{-Spy})(CO)_7(P(n\text{-Bu})_3)_2]^-} + CO \quad (4)$$

The reactions 1, 2, and 3 are first-order in complex and first-order in ligand concentrations (Figure 2). Plots of observed rate constants vs ligand concentrations yield the second-order rate constants. Second-order rate constants and activation parameters for the addition of P(*n*-Bu)$_3$ and PPh_3 to the clusters are included in Tables 1 and 2, respectively.

The trappable intermediate adduct species PPN[$Ru_3(\mu_3\text{-}\eta^2\text{-PhNpy})(CO)_9(PPh_3)$] (**4b**) obtained from the 2-anilinopyridyl derivative **1** was found to lose either PPh_3 or a CO ligand (eqs 5 and 6) to give a mixture of the starting antecedent species **1** and its monosubstituted derivative.

$$[Ru_3(\mu\text{-}\eta^2\text{-PhNpy})(CO)_9(PPh_3)]^- \rightarrow \underset{\mathbf{4b}}{} \underset{\mathbf{1}}{[Ru_3(\mu_3\text{-}\eta^2\text{-PhNpy})(CO)_9]^-} + PPh_3 \quad (5)$$

$$[Ru_3(\mu\text{-}\eta^2\text{-PhNpy})(CO)_9(PPh_3)]^- \rightarrow \underset{\mathbf{4b}}{} \underset{\mathbf{5b}}{[Ru_3(\mu_3\text{-}\eta^2\text{-PhNpy})(CO)_8(PPh_3)]^-} + CO \quad (6)$$

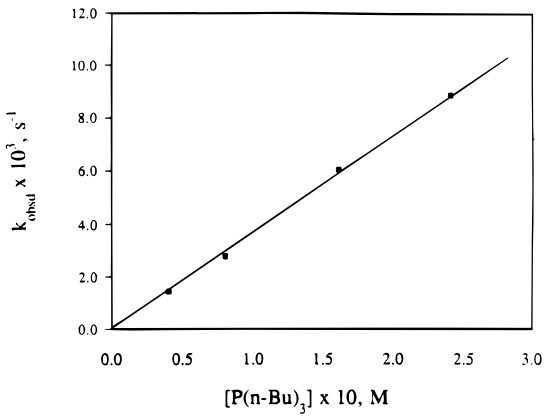

Figure 2. Plot of the observed rate constants vs ligand concentrations for the reaction of [PPN][$Ru_3(\mu_3\text{-}\eta^2\text{-Spy})(CO)_9$] (**3**) with P(*n*-Bu)$_3$ (eq 3) at 12.4 °C in THF.

Table 1. Second-Order Rate Constants and Activation Parameters for Reactions of [PPN][$Ru_3(\mu_3\text{-}\eta^2\text{-Xpy})(CO)_9$] with P(*n*-Bu)$_3$ (Eqs 1−3) in THF

Xpy	T (°C)	10^2k_2 (s^{-1} M^{-1})	$\Delta H^\ddagger$ (kcal/mol)	$\Delta S^\ddagger$ (cal/mol K)
PhNpy	−10.8	2.19	8.3 ± 1.2	−34.3 ± 4.2
	−1.0	3.64		
	10.5	7.84		
	15.0[a]	9.05		
MeNpy	5.0	0.987	8.8 ± 0.8	−36.4 ± 2.7
	15.0	1.65		
	25.5	3.09		
Spy	3.5	2.44	8.7 ± 1.2	−34.4 ± 4.3
	12.4	3.76		
	23.2	7.47		
	15.0[a]	4.29		

[a] Estimated values.

Table 2. Second-order Rate Constants and Activation Parameters for Reactions of [PPN][$Ru_3(\mu_3\text{-}\eta^2\text{-PhNpy})(CO)_9$] with PPh_3 and P(*n*-Bu)$_3$ (Eq 1) in THF

phosphine	T (°C)	10^3k_2 (s^{-1})	$\Delta H^\ddagger$ (kcal/mol)	$\Delta S^\ddagger$ (cal/mol K)
PPh_3	24.5	1.11	14.3 ± 0.7	−24.2 ± 2.4
	35.0	2.74		
	44.5	5.39		
P(*n*-Bu)$_3$	35.0	269[a]	8.3 ± 1.2	−34.3 ± 4.2

[a] Estimated value.

Discussion

The second-order kinetics and low activation enthalpies as well as very negative activation entropies (Table 1) for the reactions (eqs 1−3) are consistent with an associative mechanism. One might argue that a second-order rate law is also consistent with a mechanism in which there is a pre-equilibrium of bridge opening and closing, followed by rapid addition of the entering ligand to form the initial addition product.

Scheme 1

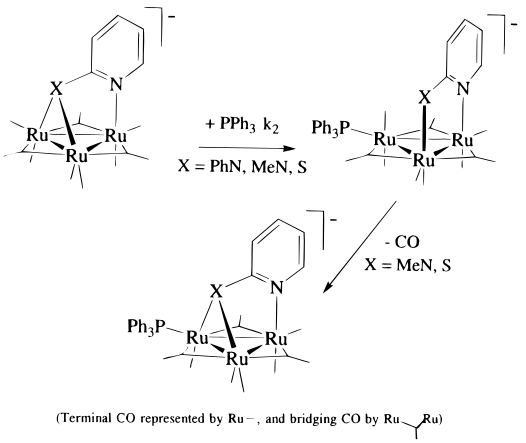

Table 3. Infrared CO-Stretching Frequencies of [PPN][$Ru_3(\mu$-η^2-Xpy)$(CO)_9$] in THF

X-py	ν(CO), cm^{-1}
PhNpy	2023 (ms), 1976 (s), 1972 (sh), 1931 (m), 1911 (m), 1790 (s)
MeNpy	2021 (ms), 1974 (s), 1971 (sh), 1929 (m), 1909 (m), 1787 (s)
Spy	2024 (ms), 1979 (s), 1970 (sh), 1932 (m), 1908 (m), 1794 (s)

However, this seems unlikely considering the low activation enthalpies for the reaction with P(n-Bu)$_3$. If the pre-equilibrium mechanism were correct, the activation enthalpy would be a sum of the bond energy of the metal-bridging ligand and the activation barrier for the entering ligand to attack the metal. The experimental values (8−9 kcal/mol, Table 1) are too low for such a reaction pathway. Further support for an associative mechanism is the fact that PPh_3 reacts with the anilinopyridyl complex **1** about 100 times slower than does P(n-Bu)$_3$, due in large part to its higher activation enthalpy (Table 2). Complexes **2** and **3** do not react with PPh_3 after 2 days, while they both react rapidly with P(n-Bu)$_3$. Such a high discrimination of metal complexes toward different ligands is often observed for associative ligand substitution reactions.[10] Thus, it is proposed that the reactions (eqs 1−3) take place *via* an associative mechanism (Scheme 1), in which a nucleophilic attack by the phosphine ligand on the metal atom is accompanied by cleavage of a Ru−X bridge bond to form an adduct in which the N (amido) or S (thiolato) donor atom of the Xpy group is bound to the metal in the terminal position (structural type **II**, *vide supra*). This is then followed by an intramolecular CO loss from the adduct to yield the monosubstituted complex.

Although the differences in rates for the reactions (eqs 1−3) are small (Table 1), experimental results do show the rates increase in the order MeNpy < Spy < PhNpy. That the 2-(methylamino)pyridyl complex is less reactive than the 2-anilinopyridyl complex is consistent with the order of electron-donating abilities of the ligands, as indicated by the CO-stretching frequencies of their complexes (Table 3). The stronger the ligand basicities, the stronger the Ru → CO π-back bonding, and the lower the CO-stretching frequencies. The lower CO-stretching frequencies of the 2-(methylamino)pyridyl complex reflect a higher electron density on the metal atoms compared to that of the 2-anilinopyridyl complex. A higher electron density on the metal atom would retard nucleophilic attack of the phosphine ligands in an associative reaction. Although the observation of an increase in the rates of these associative reactions with increasing values of ν_{CO} is consistent with what is generally found,[10] the opposite trend is observed in the case of complexes involving Spy and PhNpy as ancillary ligands. The Spy cluster has slightly higher CO stretches (Table 3), though it reacts a little slower than does the PhNpy compound. However, we wish to point out that the differences in CO-stretching frequencies are very small, as are the differences in reaction rates. Other factors may then slightly alter the rates, causing them not to conform to the normal trend. One reviewer suggests "surely there must be strain effects on the bridges that could be dominant".

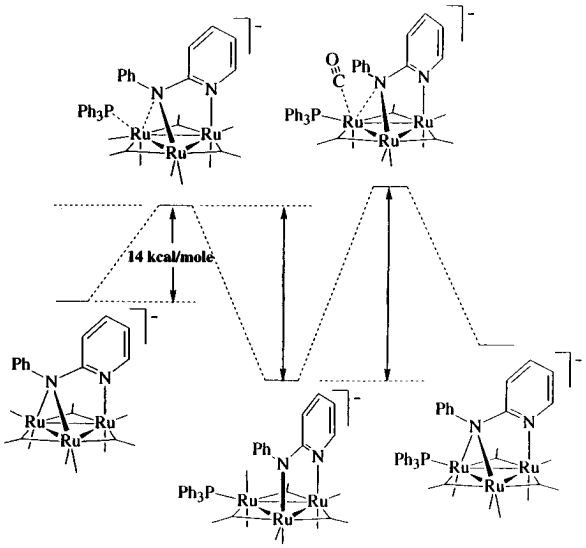

Figure 3. Reaction profile for the reaction of [PPN][$Ru_3(\mu_3$-η^2-PhNpy)$(CO)_9$] (**1**) with PPh_3 in THF.

It is noteworthy that comparable electronic effects of the 2-substituted pyridyl ligands on their complexes result in the formation of different final products obtained from these reactions under the same experimental conditions. For example, complex **1** only forms an adduct in which the anilinopyridyl ligand is bound in the μ-η^2-mode. The weak nucleophilicity of the anilinopyridyl ligand in adduct **4** does not allow it to substitute a CO ligand by forming a new N−Ru bond. On the other hand, the 2-(methylamino)pyridyl ligand is a strong enough nucleophile to displace a CO ligand after addition of P(n-Bu)$_3$ to produce the monosubstituted product **5a**. This monosubstituted derivative cannot be attacked by a second P(n-Bu)$_3$, since replacement of CO by P(n-Bu)$_3$ imparts more electron density on the cluster. The 2-thiopyridyl ligand is in the middle of this nucleophilicity trend. Indeed, its monosubstituted complex can further react with another P(n-Bu)$_3$ molecule to form the disubstituted complex.

Although we were unable to quantify the rates of PPh_3 and of CO loss from the addition product (eqs 5 and 6), spectral changes during the intramolecular ligand loss clearly shows qualitatively that PPh_3 is more readily lost than is CO. This is in accord with the departure of PPh_3 creating a less electron rich and less sterically crowded environment around the metal than does the departure of CO, which would then favor the formation of a bridging metal−ligand bond.

The above observations and the results of the kinetic study allow us to establish a reaction profile (Figure 3) illustrating the overall reaction pathway for the replacement of CO by PPh_3 in the anilinopyridyl complex **1** (eq 7).

$$[Ru_3(\mu\text{-}\eta^2\text{-PhNpy})(CO)_9]^- + PPh_3 \rightarrow [Ru_3(\mu_3\text{-}\eta^2\text{-PhNpy})(CO)_8(PPh_3)]^- + CO \quad (7)$$

As shown in Figure 3, the energy barrier for PPh_3 addition to PPN[$Ru_3(\mu_3$-η^2-PhNpy)$(CO)_9$] (**1**) is ∼14 kcal/mol. Further

(10) (a) Basolo, F. *Polyhedron* **1990**, *9*, 1503. (b) Atwood, J. D. *Inorganic and Organometallic Reaction Mechanisms*; Brooks/Cole: Monterey, CA, 1985.

ligand substitutions of CO or PPh_3 by the amido group have *higher energy barriers than the first step*. Thus, the intermediate addition product **4b** was intercepted in that case. On the other hand, MeNpy and Spy are both stronger nucleophiles than is PhNpy. Thus, intramolecular CO displacement by these ancillary ligands in the phosphine adducts has a lower energy barrier than that of the former addition reaction, thereby favoring the formation of the substituted complexes **5** and **6** as the final products.

Acknowledgment. The authors thank Northwestern University and the CNRS for support of this research.

Supporting Information Available: Observed rate constants, k_{obsd}, for reactions of eqs 1−3 (Table 1) and the total rate constants, $k_5 + k_6$, for the intramolecular ligand substitutions of eqs 5 and 6 (Table 2) (3 pages). Ordering information is given on any current masthead page.

IC950947F